Journal of Medicinal Chemistry

Article

pubs.acs.org/jmc

Structure–Activity Relationships of Targeted $Ru^{II}(\eta^6$-*p*-Cymene) Anticancer Complexes with Flavonol-Derived Ligands

Andrea Kurzwernhart,[†] Wolfgang Kandioller,[†,‡] Simone Bächler,[§] Caroline Bartel,[†] Sanela Martic,[∥] Magdalena Buczkowska,[⊥] Gerhard Mühlgassner,[†] Michael A. Jakupec,[†,‡] Heinz-Bernhard Kraatz,[∥] Patrick J. Bednarski,[⊥] Vladimir B. Arion,[†] Doris Marko,[§] Bernhard K. Keppler,[†,‡] and Christian G. Hartinger*[,†,‡,#]

[†]Institute of Inorganic Chemistry, University of Vienna, Waehringer Strasse 42, 1090 Vienna, Austria

[‡]Research Platform "Translational Cancer Therapy Research", University of Vienna, Waehringer Strasse 42, 1090 Vienna, Austria

[§]Institute of Food Chemistry and Toxicology, University of Vienna, Waehringer Strasse 38, 1090 Vienna, Austria

[∥]Department of Physical and Environmental Sciences, University of Toronto, Scarborough, Canada

[⊥]Department of Pharmaceutical and Medicinal Chemistry, University of Greifswald, 17487 Greifswald, Germany

[#]The University of Auckland, School of Chemical Sciences, Private Bag 92019, Auckland 1142, New Zealand

Supporting Information

ABSTRACT: Ru^{II}(arene) complexes have been shown to be promising anticancer agents, capable of overcoming major drawbacks of currently used chemotherapeutics. We have synthesized $Ru^{II}(\eta^6$-arene) compounds carrying bioactive flavonol ligands with the aim to obtain multitargeted anticancer agents. To validate this concept, studies on the mode of action of the complexes were conducted which indicated that they form covalent bonds to DNA, have only minor impact on the cell cycle, but inhibit CDK2 and topoisomerase IIα in vitro. The cytotoxic activity was determined in human cancer cell lines, resulting in very low IC_{50} values as compared to other Ru^{II}(arene) complexes and showing a structure–activity relationship dependent on the substitution pattern of the flavonol ligand. Furthermore, the inhibition of cell growth correlates well with the topoisomerase inhibitory activity. Compared to the flavonol ligands, the $Ru^{II}(\eta^6$-*p*-cymene) complexes are more potent antiproliferative agents, which can be explained by potential multitargeted properties.

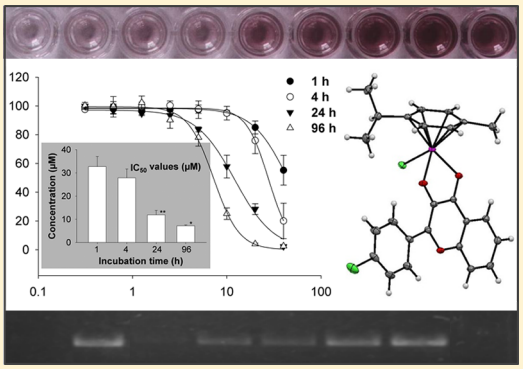

INTRODUCTION

Metallodrugs have become important compounds in cancer therapy, and, in particular, platinum complexes are used worldwide against many tumor types.[1] To overcome severe side effects and drug resistance during treatment, which are their major drawbacks,[2] complexes with metal ions other than platinum have become the focus of research.[1] Especially, ruthenium complexes offer a number of interesting properties such as lower toxicity and a range of physiologically accessible oxidation states.[3] The Ru^{III} complexes NAMI-A and KP1019 have shown the most promising results in preclinical and clinical studies (Chart 1).[4−6] The more selective activity of these compounds due to an efficient uptake as protein adducts and activation by reduction inside the tumor is thought to be responsible for the low general toxicity.[4] During the last years, organometallic Ru^{II} complexes, especially half-sandwich Ru^{II}(arene) compounds, moved into the focus of interest because biological activity and pharmacological properties can easily be modulated by ligand selection. Important examples of this compound type comprise the RAPTA family[7] (Chart 1) containing the pta ligand (1,3,5-triaza-7-phosphatricyclo-[3.3.1.1]decane) and Ru^{II}(arene) complexes of bidentate ethylenediamine, which are at an advanced preclinical development stage.[8]

Chart 1. Chemical Structures of KP1019, NAMI-A, and RAPTA-C

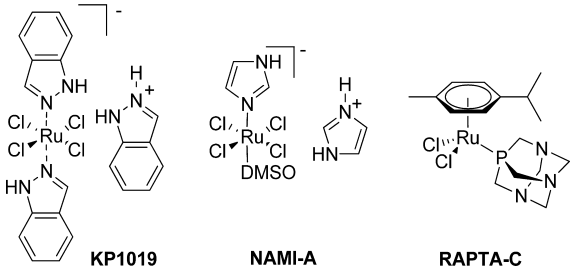

The RAPTA complexes are a good example of organometallics which can be equipped with ligands to obtain desired

Received: July 30, 2012
Published: November 7, 2012

dx.doi.org/10.1021/jm301376a | J. Med. Chem. 2012, 55, 10512−10522

properties. Whereas the parent compound RAPTA-C is a metastasis inhibitor, tethering the organometallic fragment to ethacrynic acid resulted in compounds with glutathione-*S*-transferase inhibitory activity, accompanied by a cleavage of the enzyme inhibiting moiety from the metal fragment which can target a second biomolecule, e.g., DNA. This concept of multitargeted anticancer agents, i.e., drugs designed to act against several individual molecular targets, offers a number of advantages over classic chemotherapeutics, including tunable pharmacological properties and anticancer activity and altered metabolism and resistance development.[9] Such drugs can be prepared by linking metal fragments to biologically active ligand systems and, as shown in the RAPTA case, by functionalization of an arene ligand or, as previously reported by us, by direct coordination of 3-hydroxyflavones to a Ru^{II}(cym) moiety (cym = η^6-*p*-cymene).[10]

Flavonoids are known as natural components of plants, fruits, and vegetables and exhibit interesting biological properties such as antioxidant, anti-inflammatory, estrogenic, antimicrobial, and anticarcinogenic activity.[11−13] The 3-hydroxy-4-keto motif of 3-hydroxyflavones offers facile coordination to many metal ions. The resulting metal complexes exhibit high stability constants, high molar absorbances, and fluorescence properties and are biocompatible.[14,15] Therefore, such compounds have been investigated as new fluorochromic indicators for ion chelation and biomembrane structure studies in the human body.[16] In addition, a few examples of tumor-inhibiting metal−flavonoid complexes are known.[17]

Herein, we report a series of Ru^{II}(cym) complexes with 3-hydroxyflavone ligands with the aim to study the influence of the substituent on the phenyl ring of the ligand on the anticancer activity. To support the hypothesis of multitargeted compounds, their behavior in aqueous solution and in the presence of nucleotides was studied. Furthermore, the inhibition of cyclin-dependent kinases (CDKs) and their effect on the cell cycle has been assayed, as well as their human topoisomerase IIα inhibitory activity.

RESULTS AND DISCUSSION

We have extensively studied the application of *O*,*O*-chelating hydroxypyrone complexes as potential anticancer agents and recently extended these investigations to 3-hydroxyflavones with the same binding motif.[10] To establish structure−activity relationships (SAR), a series of derivatives was synthesized in two steps, starting with a Claisen−Schmidt condensation of 2-hydroxyacetophenone **1** and benzaldehydes **a**−**j** in alkaline solution. In the second step, the obtained 2′-hydroxychalcones were converted into the respective 3-hydroxyflavones **2a**−**j** under Algar−Flynn−Oyamada reaction conditions with hydrogen peroxide and NaOH (Scheme 1).[18−20] The Ru^{II}(cym) complexes **3a**−**j** were synthesized by deprotonation of **2a**−**j** with sodium methoxide and subsequent reaction with bis[dichlorido(η^6-*p*-cymene)ruthenium(II)] (Scheme 1).[21] All complexes were obtained in moderate to good yields (30−68%) and are stable for more than one year, even if exposed to sunlight and air, which was confirmed by NMR spectroscopy and elemental analysis.

All synthesized compounds were characterized by standard methods (see Experimental Section), and single crystals of **3d**, **3f**, and **3h** were analyzed by X-ray diffraction methods (Figure 1) and are compared to **3b**.[10] Complex **3d** crystallizes in the centrosymmetric space group $P\bar{1}$ and **3f** and **3h** in the monoclinic space group $P2_1/n$. The compounds feature the

Scheme 1. Synthesis of 3-Hydroxyflavone Ligands and their $Ru^{II}(\eta^6$-*p*-Cymene) Complexes

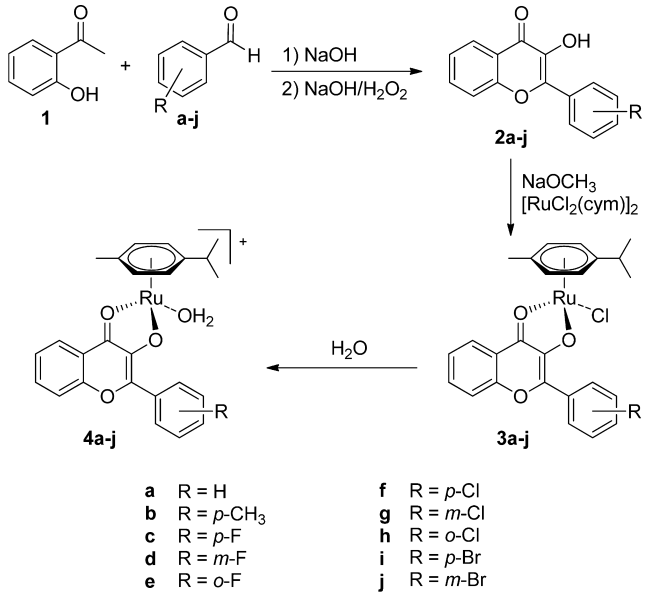

pseudo-octahedral "piano-stool" configuration similar to related Ru^{II}(cym) complexes.[10,22] The 3-hydroxyflavone acts as a bidentate ligand, forming a nonplanar, envelope-like five-membered metallocycle. The phenyl substituent of the ligand is twisted with a torsion angle of 48.4(4)° in **3h**, but only 5.1(3)° in **3f**, 0.2(3)° in **3d**, and 15.3(6)° in **3b**. The two Ru−O bonds were found to be slightly different as in **3b** with 2.0664(14) and 2.1154(14) Å in **3d**, 2.0747(11) and 2.1098(11) in **3f**, and 2.0870(16) and 2.1339(16) Å in **3h**, which is in accordance to Ru−O bonds in similar compounds.[23,24] The Ru−Cl bonds [2.4105(5) Å (**3d**), 2.4132(4) (**3f**), and 2.4100(7) Å (**3h**)] are in the range of recently published Ru^{II}(cym) complexes [2.4200(11)−2.4273(8) Å][4−7,10] but shorter than in **3b** with 2.4326(10). The Ru−$cym_{centroid}$ distances were found at 1.638 for both **3d** and **3f** and at 1.647 Å for **3h**.

The aqueous stability of the complexes was studied by ^{1}H NMR spectroscopy (Figure 2). Dissolution of organometallic Ru(arene) compounds featuring an *O*,*O*-chelating motif and a halido ligand often results in rapid exchange of the chlorido ligand by an aqua moiety.[25] The same behavior was demonstrated for such complexes which aquated within seconds, leading to charged **4a**−**c**, **4f**, and **4i** (Scheme 1).[26,27] The hydrolyzed compounds are relatively stable in aqueous solution for about 24 h, however, after 6 days, the formation of the dimeric hydrolysis side product $[Ru_2(cym)_2(OH)_3]^+$ was clearly visible in ESI-mass and NMR spectra. This species does not affect the cytotoxic activity as it is thermodynamically stable and unreactive toward nucleophiles.[25,28] Notably, **3a**−**j** exhibit approximately 10-fold better solubility in water than the respective ligands, e.g., 0.03 mg/mL for **2a** and 0.3 mg/mL for **3a** in 1% DMSO/H_2O.

Cytotoxic Activity. The in vitro anticancer activity was determined in the human cancer cell lines CH1 (ovarian carcinoma), SW480 (colon carcinoma), and A549 (non-small cell lung carcinoma) by means of the colorimetric MTT assay and in human urinary bladder (5637), human large cell lung (LCLC-103H), and human pancreatic carcinoma cell lines (DAN-G) with the crystal violet assay, both after 96 h.

dx.doi.org/10.1021/jm301376a | J. Med. Chem. 2012, 55, 10512−10522

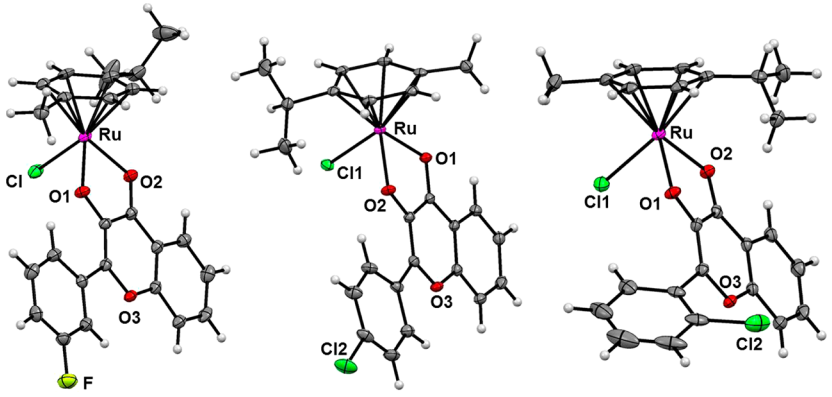

Figure 1. Molecular structures of the Ru^{II}(cym) complexes **3d** (left), **3f** (center), and **3h** (right).

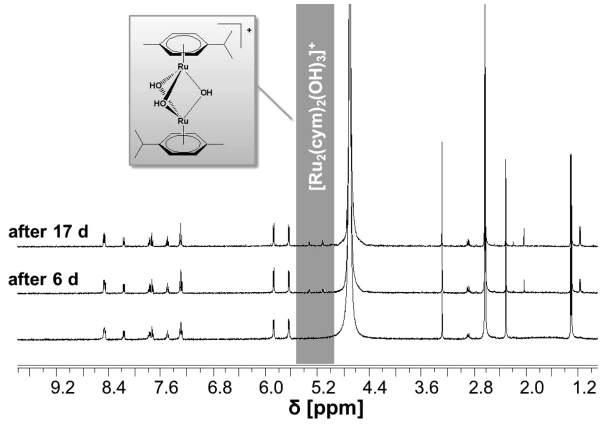

Figure 2. Hydrolysis of **3c** in 10% DMSO-d_6/D_2O studied by ^1H NMR spectroscopy. After 6 d, the formation of the dimeric hydrolysis side product $[Ru_2(cym)_2(OH)_3]^+$ was observed giving signals at 5.1 and 5.3 ppm.

In general, the biological activity as determined by the MTT assay and given as the IC_{50} values (50% inhibitory concentration; Table 1) was in the low micromolar range, which is very unusual for Ru^{II}(arene) compounds, and only a few more examples with similar cytotoxicity are known.[4,29,30] The chemosensitive CH1 cell line was most sensitive to the test compounds with IC_{50} values lower than 7.9 μM, followed by SW480 with IC_{50} values ranging from 3.4−26 μM. The lowest cytotoxic potency was found for the generally more chemo-resistant A549 cells. In comparison to compound **3a** with an unsubstituted ligand structure, *ortho* substitution of the phenyl ring (**3e** and **3h**) appears unfavorable, whereas *meta* and *para* substitution (**3f**, **3g**, **3i**) increases the anticancer activity. This may be due to a structural effect, as the phenyl ring is considerably more twisted in the *ortho* derivative than in the *meta*- and *para*-substituted compounds (Figure 1), which may influence the interaction with biological targets.[31] However, the type of substituent, whether electron-withdrawing or electron-donating, seems to be of minor importance, whereas their position appears to be crucial for the cytotoxic activity. We have shown earlier that the ligands are the bioactive moiety, which is mainly responsible for the antiproliferative activity.[10] However, they are poorly soluble in aqueous solutions and therefore hardly suitable for pharmaceutical applications.

The crystal violet assay for antiproliferative activity in the 5637, the LCLC-103H, and the DAN-G cell lines (Table 1) revealed slightly higher IC_{50} values than that for the MTT assay in the CH1 cell line but still notable for Ru^{II}(arene) complexes. Compounds **3d** and **3f** exhibit the lowest IC_{50} values at around 5 μM in these three cell lines and also show the highest potency in the MTT assays. Their antiproliferative activity is in the same range as that of related dinuclear Ru(arene)(pyridone) compounds.[32] Compounds **3b** and **3d** show the best overall activity in the used cell lines. However, some compounds are more specific for one of the three cell lines used in the crystal violet assays, e.g., **3i** for DAN-G, **3f** and **3j** for 5637, and **3c** and **3g** for LCLC-103H, which is a highly desirable characteristic for anticancer agents.[32,33]

Table 1. In Vitro Anticancer Activity of 3a−j (96 h Exposure) in Human Ovarian, Colon, Non-Small Cell Lung, Urinary Bladder, Large Cell Lung, and Pancreatic Carcinoma Cell Lines (Mean Values ± SD of Three Independent Determinations unless Otherwise Noted)

	IC_{50} values/μM					
compd	CH1	SW480	A549	5637	LCLC-103H	DAN-G
3a	2.1 ± 0.2	9.6 ± 1.5	20 ± 2	11 ± 5	13 ± 6	12 ± 2
3b	1.8 ± 0.2	7.2 ± 0.5	17 ± 2	5.7 ± 3.2	5.2 ± 0.8	6.6 ± 2.5
3c	1.7 ± 0.4	7.9 ± 2.0	18 ± 1	33 ± 5	5.5 ± 5.2	12 ± 2
3d	1.5 ± 0.1	7.0 ± 1.0	15 ± 1	4.3 ± 2.5	4.3 ± 1.1	5.3 ± 1.6
3e	4.0 ± 0.8	24 ± 3	30 ± 1	nd	nd	nd
3f	0.86 ± 0.06	3.8 ± 0.5	9.5 ± 0.5	3.3 ± 1.1	13 ± 1	19 ± 7
3g	1.0 ± 0.1	7.0 ± 0.7	12 ± 2	30 ± 2	5.0 ± 3.5	19 ± 5
3h	7.9 ± 0.6	26 ± 1	51 ± 5	nd	nd	nd
3i	1.2 ± 0.2	3.4 ± 0.1	8.6 ± 0.7	12 ± 1	19 ± 6	5.7 ± 1.9
3j	2.3 ± 0.7	7.2 ± 0.4	17 ± 3	5.9 ± 1.2	16 ± 4	20 ± 5

dx.doi.org/10.1021/jm301376a | J. Med. Chem. 2012, 55, 10512−10522

Furthermore, the time dependence of the cytotoxicity of **3j** was investigated and the IC_{50} values of **3j** were determined after 1, 4, 24, and 96 h in SW480 cells (Figure 3). The calculated IC_{50} values for **3j** decreased from about >40 μM after 1 h to 12 μM after 24 h and finally to 7 μM after 96 h.

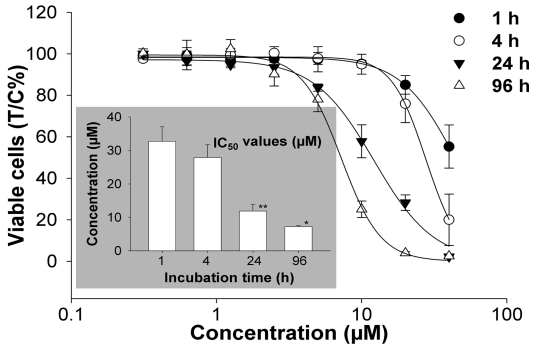

Figure 3. Time-dependent anticancer activity of **3j** in SW480 cells. Significances indicated refer to the next shorter incubation time calculated by Student's *t* test (*p < 0.1, **p < 0.05).

Inhibition of CDK2. The anticancer activity of the flavonoid flavopiridol is linked to its inhibition of cyclin-dependent kinases (CDKs),[34] and therefore this group of proteins is also a possible target for Ru–flavonoid complexes. To estimate the compounds' potential to inhibit kinases, the inhibition of CDK2 was studied by an electrochemical assay employing Fc-ATP as a cosubstrate in the kinase phosphorylation reaction.[35,36] The peptide HHASPRK was used as a substrate and immobilized onto the Au surface for the study of CDK2/cyclin A protein kinase activity. Following the kinase-catalyzed Fc-phosphorylation reaction, the Fc group is transferred from Fc-ATP to the immobilized peptide and results in an electrochemical signal. Hence, the electrochemical readout is directly related to the extent of Fc-phosphorylation by a protein kinase. In general, the Fc-phosphorylations are monitored by square-wave voltammetry wherein the oxidation peak at ~440 ± 5 mV signals the successful Fc-phosphorylation. The dependence of the integrated current density in CDK2/cyclin A kinase assays as a function of inhibitors **3a–h** (10 μM) is shown in Figure 4. With the exception of **3c** and **3f**, all compounds inhibit CDK2 in about the same range as structurally related HOPO complexes[37] and are nearly as active as the well-known CDK2 inhibitor roscovitine (R), which was included for comparison (Figure 4). It appears that *para* substituents at the phenyl ring of the flavone ligands are less favorable than *ortho* and *meta* substitution. However, no direct structure–activity relationships can be derived when compared to the in vitro anticancer activity data set. Therefore, considering also the minor influence on the cell cycle (see below), CDK2 and CDKs in general are not considered as the main target of this type of compounds.

Impact on the Cell Cycle. The cell cycle distribution of A549 cells was studied by treating exponentially growing A549 cells with **3a–c** and **3e** in various concentrations for 48 h. Then cells were stained with propidium iodide and analyzed for their DNA content by flow cytometry. The four Ru compounds have comparable effects on the cell cycle, most probably due to their similar structures. The effects vary in dependence of the concentration (Figure 5). Low concentrations (<32 μM of **3a**, **3b**, and **3c** and <16 μM of **3e**) induce a slight G_2/M arrest,

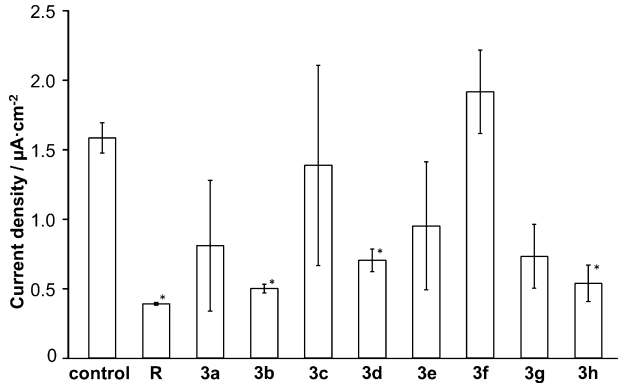

Figure 4. Integrated current densities (estimated from square-wave voltammograms) observed in CDK2/cyclin A kinase-catalyzed Fc-phosphorylation of the surface bound peptide in the presence of the organometallic compounds (**3a–3h**) and compared to roscovitine (R) (inhibitor concentration = 10 μM, 100 mV/s scan rate, 0.1 M phosphate buffer pH 7.4 electrolyte, triplicate measurements). Significances indicated refer to the control calculated by Student's *t* test (*p < 0.1, **p < 0.05).

accompanied by a decrease of the G_0/G_1-phase fraction, whereas at higher concentrations these effects tend to level out again. The impact on the S phase is less pronounced, but a slight increase can be observed at increasing concentrations of **3b**, **3c**, and especially **3f** (>16 μM, Figure 5). These results indicate that CDK2 is not very likely to be an intracellular target because this kinase is involved in the G1/S transition of the cell cycle, which is not influenced in a dose-dependent manner by the Ru complexes studied.

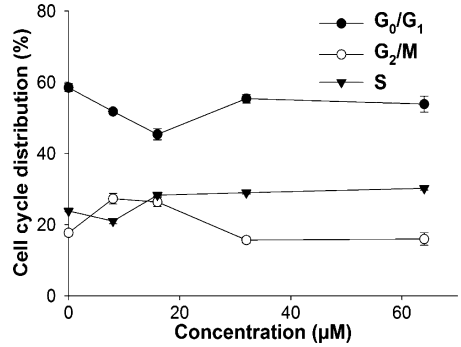

Figure 5. Concentration-dependent impact of **3f** on the cell cycle distribution of A549 cells after exposure for 48 h (values are means ± standard deviations of two independent experiments).

Topoisomerase Inhibition. Topoisomerases are overexpressed in many types of cancer and thus are major targets for antineoplastic agents such as doxorubicin, etoposide, and mitoxantrone.[38,39] Flavonoids are also known to inhibit human topoisomerases,[40,41] which are enzymes that change the topology of DNA by introducing a transient break in the DNA strand, allowing a second DNA region from either the same molecule (relaxation, knotting, or unknotting) or a different molecule (catenation or decatenation) to pass through. During this process, the enzymes are covalently bound to the DNA via an active tyrosine residue, termed "cleavable complex". After the DNA is untangled or unwound, the strands are reannealed by the enzyme so that the overall composition of the DNA strand does not change. DNA

dx.doi.org/10.1021/jm301376a | J. Med. Chem. 2012, 55, 10512–10522

topoisomerases are participating in nearly all biological processes involving DNA including replication, transcription, recombination, and chromatin remodeling.[42,43] They are classified as type I and type II depending on if they induce single- or double-strand breaks, respectively.

In the case of topoisomerase inhibitors, an increase of the proportion of cells in the S-phase and at higher concentrations a G2/M arrest are expected. In the case of the Ru complexes studied here, a slight increase in the S-phase fraction was observed (Figure 5) and therefore topoisomerase inhibition studies were conducted. The catalytic activity of topoisomerase IIα is determined by means of the decatenation assay. Catenated kinetoplast DNA (kDNA) consists of interlocked DNA minicircles (mostly 2.5 kb), which can be released to single DNA circles by catalytically active topoisomerase II. If topoisomerase II is inhibited, kDNA stays in its catenated form, which is not able to enter the agarose gel, whereas the single DNA circles, released by topoisomerase II, are able to migrate into the gel (Figure 6, compare lane 1 with lane 2). Thus,

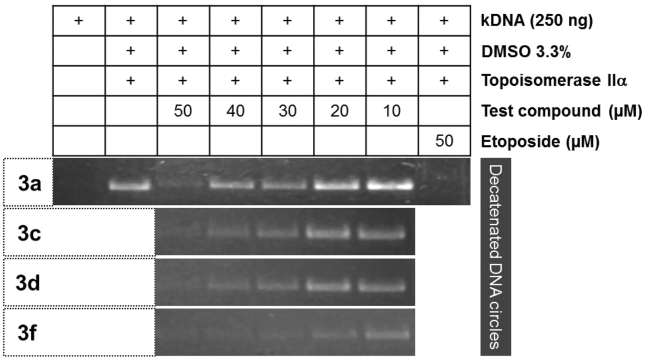

Figure 6. Concentration-dependent effect of the Ru complexes **3a**, **3c**, **3d**, and **3f** on the catalytic activity of topoisomerase IIα, as determined by the decatenation assay. The topoisomerase poison etoposide was used as a control.

kDNA was incubated with topoisomerase IIα in the presence of different concentrations of the Ru^{II}(cym) complexes **3a**−**3d**, **3f**, **3g**, **3i**, and **3j** and the flavonols **2a**−**c**, **2f**, and **2i**. All complexes inhibit the catalytic activity of human topoisomerase IIα at concentrations $\geq$10 μM. The extent of inhibition appears to be well correlated to their in vitro anticancer potency, with **3f** being the most potent inhibitor followed by **3d** (Figure 6), and with **3a** as the least cytotoxic and weakest inhibitor of topoisomerase IIα. Compared to the flavonols, their Ru^{II}(cym) complexes are more potent in all studied cases, demonstrating that the inhibition of topoisomerase IIα is enhanced by the linkage of the topoisomerase-inhibiting flavonoid scaffold to the Ru^{II}(cym) moiety. We explain this observation by multitargeted properties of the complexes, as they are also able to interact with the DNA.[10]

Nucleotide Binding. To help estimate the reactivity to DNA, the interaction of the aqua species **4a**−**c**, **4f**, and **4i** with the DNA model compound 5′-GMP was investigated by ^{1}H NMR spectroscopy. The 5′-GMP N7-adducts were formed immediately, as indicated by an upfield shift of the *H*8 signal of 5′-GMP from approximately δ = 8.1 to 7.6 ppm.[10,44] Therefore, DNA represents a suitable binding partner for this class of compounds.

CONCLUSIONS

Flavonoids exhibit interesting biological properties, and members of this compound class have been investigated in clinical trials as anticancer agents. By combining such moieties with metal fragments, we aimed to obtain anticancer agents that can interact with more than one target, facilitating single-molecular combination therapy. A series of light- and air-stable Ru^{II}(η^6-*p*-cymene) complexes with flavonol ligands were prepared in good yields. The flavonol ligands **2a**−**j** are hardly soluble in aqueous solutions, which prevents their potential use as anticancer agents. In contrast, the Ru^{II}(cym) complexes **3a**−**j** exhibit approximately 10-fold better solubility in water than the ligands. However, they aquate within seconds by an exchange of the chlorido ligand with an aqua moiety, leading to **4a**−**j**, which are then able to bind to DNA, as shown for the DNA model compound 5′-GMP. The flavonol-derived compounds exhibit IC_{50} values in the low μM range, which is unusual for Ru^{II}(cym) complexes, but this indicates the central role of the ligand system as the anticancer activity determining factor. This is also highlighted by comparison of the IC_{50} values of the coordination compounds and the respective ligand systems.[10] Complexes **3f**, **3g**, and **3i** with *para*- and *meta*-substituted ligands exhibit lower IC_{50} values than their unsubstituted analogue **3a** or the *ortho*-substituted derivatives **3e** and **3h**.

To gain information on the mode of action of the complexes and in light of the biological properties of the ligands, the inhibitory activity of the complexes on topoisomerase IIα and CDK2 was assayed and flow cytometry analyses of the cell cycle were conducted. These studies revealed that **3a**−**c** and **3e** have an influence on the cell cycle distribution, and especially at concentrations around the IC_{50} values of the compounds, an increase in the cell fraction in G_0/G_1 phase was observed. Furthermore, most of the complexes were shown to inhibit CDK2 to an extent approaching that of roscovitine, a well-known CDK2 inhibitor. However, these results did not resemble the activity pattern observed in the in vitro anticancer assays. Notably, the inhibition of topoisomerase IIα correlated well with the in vitro anticancer activity data, with the compounds exhibiting the lowest IC_{50} values in the MTT assay being also the most potent topoisomerase IIα inhibitors. Compared to the unsubstituted flavonol ligands **2a**−**j**, which are considered as the topoisomerase-inhibiting moiety in the coordination compound, the respective Ru^{II}(cym) complexes **3a**−**j** are shown to inhibit topoisomerase IIα to a greater extent. This may be explained by their additional ability to form bonds to the DNA base guanine and thereby acting in a bifunctional manner, which could be beneficial in tumor therapy.

EXPERIMENTAL SECTION

All solvents were dried and distilled prior to use. 2-Hydroxyacetophenone **1** (Fluka, Acros Organics), benzaldehyde **a** (Fluka), 4-tolualdehyde (Acros Organics), 4-fluorobenzaldehyde **c** (Fluka), 3-fluorobenzaldehyde **d** (Fluka), 2-fluorobenzaldehyde **e** (Fluka), 4-chlorobenzaldehyde **f** (Acros Organics), 3-chlorobenzaldehyde **g** (Aldrich), 2-chlorobenzaldehyde **h** (Aldrich), 4-bromobenzaldehyde **i** (Aldrich), 3-bromobenzaldehyde **j** (Aldrich), ruthenium(III) chloride (Johnson Matthey), α-terpinene (Acros Organics), and sodium methoxide (Aldrich) were purchased and used without further purification. Bis[(η^6-*p*-cymene)dichloridoruthenium(II)] was synthesized as described elsewhere.[45]

Melting points were determined with a Büchi melting point B-540 apparatus. Elemental analyses were carried out with a Perkin-Elmer 2400 CHN elemental analyzer by the Microanalytical Laboratory of the University of Vienna. NMR spectra were recorded at 25 °C using a

Bruker FT-NMR spectrometer Avance III 500 MHz. ^{1}H NMR spectra were measured at 500.10 MHz and ^{13}C{^{1}H}-NMR spectra at 125.75 MHz in DMSO-d_6 or $CDCl_3$. The 2D NMR spectra were measured in a gradient-enhanced mode.

The X-ray diffraction data for **3d**, **3f**, and **3h** were collected on a Bruker X8 APEX II CCD diffractometer at 100 K. The single crystals were positioned at 35, 35, and 40 mm from the detector, and 1746, 1367, and 1667 frames were measured, each for 20, 5, and 5 s over 1° scan width. The data were processed using the SAINT software package.[46] The structures were solved by direct methods and refined by full-matrix least-squares techniques. Non-hydrogen atoms were refined with anisotropic displacement parameters. H atoms were inserted at calculated positions and refined with a riding model. The following computer programs were used: structure solution, SHELXS-97; refinement, SHELXL-97;[47] molecular diagrams, ORTEP-3.[48] The crystallographic data files for **3d**, **3f**, and **3h** have been deposited with the Cambridge Crystallographic Database as CCDC 886667, 886666, and 886665, respectively.

General Procedure for the Synthesis of the 3-Hydroxyflavone Ligands 2a−2j. NaOH (5 M, 4.3 equiv) was added to a solution of 2-hydroxyacetophenone **1** (1.0 equiv) and aldehydes **a**−**i** (1.0 equiv) in ethanol, and the solution was stirred for 18 h at room temperature. The reaction mixture was acidified to pH 6 by addition of acetic acid (30%), and the 2′-hydroxychalcone was isolated by filtration. The 2′-hydroxychalcone (1.0 equiv) was suspended in ethanol, NaOH (5 M, 2.0 equiv), and H_2O_2 (30%, 2.2 equiv) were added at 4 °C. The mixture was stirred for 18 h at room temperature, afterward acidified to pH 1 with HCl (2 M) and poured onto water (400 mL). The precipitate was collected by filtration, and the pure product was obtained by recrystallization from methanol.

*3-Hydroxy-2-phenyl-chromen-4(1H)-one (**2a**).* The synthesis was performed according to the general procedure by using **1** (2.00 g, 14.7 mmol) and **a** (1.56 g, 14.7 mmol) to afford **2a** as a yellow powder (2.63 g, 75%); mp 165−168 °C. ^{1}H NMR (500.10 MHz, DMSO-d_6): δ = 7.49−7.54 (m, 2H, H4′/H7), 7.59 (dd, ^3J(H,H) = 7 Hz, ^3J(H,H) = 7 Hz, 2H, H3′/H5′), 7.79 (d, ^3J(H,H) = 7 Hz, 1H, H8), 7.83−7.81 (m, 1H, H6), 8.14 (dd, ^4J(H,H) = 1 Hz, ^3J(H,H) = 8 Hz, 1H, H5), 8.24 (d, ^3J(H,H) = 7 Hz, 2H, H2′/H6′), 9.64 (br s, 1H, OH) ppm. ^{13}C{^{1}H} NMR (125.75 MHz, DMSO-d_6): δ = 118.9 (C8), 121.8 (C8a), 125.1 (C7), 125.3 (C5), 128.1 (C2′/C6′), 129.0 (C3′/C5′), 130.4 (C4′), 131.8 (C2), 134.2 (C6), 139.6 (C1′), 145.7 (C3), 155.1 (C4a), 173.5 (C4) ppm. Elemental Anal. calcd for $C_{15}H_{10}O_3$: C 75.62, H 4.23%. Found: C 75.62, H 4.09%.

*3-Hydroxy-2-(4-methylphenyl)-chromen-4(1H)-one (**2b**).* The synthesis was performed according to the general procedure by using **1** (2.00 g, 14.7 mmol) and **b** (1.76 g, 14.7 mmol) to afford **2b** as yellow crystals (1.64 g, 44%); mp 191−194 °C. ^{1}H NMR (500.10 MHz, DMSO-d_6): δ = 2.41 (s, 3H, CH_3), 7.40 (d, ^3J(H,H) = 8 Hz, 2H, H3′/H5′), 7.47−7.50 (m, 1H, H7), 7.79 (d, ^3J(H,H) = 7 Hz, 1H, H8), 7.79−7.82 (m, 1H, H6), 8.14 (dd, ^4J(H,H) = 1 Hz, ^3J(H,H) = 8 Hz, 1H, H5), 8.16 (d, ^3J(H,H) = 8 Hz, 2H, H2′/H6′), 9.56 (br s, 1H, OH) ppm. ^{13}C{^{1}H} NMR (125.75 MHz, DMSO-d_6): δ = 21.5 (CH_3), 118.9 (C8), 121.7 (C8a), 125.0 (C7), 125.3 (C5), 128.1 (C2′/C6′), 129.1 (C2), 129.6 (C3′/C5′), 134.1 (s, C6), 139.4 (C1′), 140.3 (C4′), 145.9 (C3), 155.1 (C4a), 173.4 (C4) ppm. Elemental Anal. Calcd for $C_{16}H_{12}O_3$·0.15H_2O: C 75.37, H 4.86%. Found: C 75.38, H 4.47%.

*3-Hydroxy-2-(4-fluorophenyl)-chromen-4(1H)-one (**2c**).* The synthesis was performed according to the general procedure by using **1** (2.00 g, 14.7 mmol) and **c** (1.82 g, 14.7 mmol) to afford **2c** as yellow needles (1.65 g, 44%); mp 151−152 °C. ^{1}H NMR (500.10 MHz, DMSO-d_6): δ = 7.42−7.45 (m, 2H, H3′/H5′), 7.47−7.50 (m, 1H, H7), 7.79 (d, ^3J(H,H) = 7 Hz, 1H, H8), 7.81−7.83 (m, 1H, H6), 8.13 (dd, ^4J(H,H) = 1 Hz, ^3J(H,H) = 8 Hz, 1H, H5), 8.29−8.32 (m, 2H, H2′/H6′), 9.72 (br s, 1H, OH) ppm. ^{13}C{^{1}H} NMR (125.75 MHz, DMSO-d_6): δ = 116.1 (d, ^2J(H,H) = 22 Hz, C3′/C5′), 118.9 (C8), 121.8 (C8a), 125.1 (C7), 125.3 (C5), 128.3 (d, ^4J(C,F) = 3 Hz, C1′), 130.6 (d, ^3J(C,F) = 8 Hz, C2′/C6′), 134.2 (C6), 139.3 (C2), 144.9 (C3), 155.0 (C4a), 163.0 (d, ^1J(C,F) = 249 Hz, C4′), 173.4 (C4) ppm. Elemental Anal. Calcd for $C_{15}H_9FO_3$·0.15H_2O: C 69.58, H 3.62%. Found: C 69.66, H 3.47%.

*3-Hydroxy-2-(3-fluorophenyl)-chromen-4(1H)-one (**2d**).* The synthesis was performed according to the general procedure by using **1** (2.00 g, 14.7 mmol) and **d** (1.82 g, 14.7 mmol), affording **2d** as a yellow powder (0.89 g, 50%); mp 171−173 °C. ^{1}H NMR (500.10 MHz, DMSO-d_6): δ = 7.37 (ddd, ^4J(H,F) = 2 Hz, ^3J(H,H) = 8 Hz, ^3J(H,H) = 8 Hz, 1H, H4′), 7.48−7.51 (m, 1H, H7), 7.64 (ddd, ^4J(H,F) = 2 Hz, ^3J(H,H) = 8 Hz, ^3J(H,H) = 8 Hz, 1H, H5′), 7.81−7.86 (m, 2H, H6/H8), 8.04 (dd, ^4J(H,H) = 2 Hz, ^3J(H,H) = 11 Hz, 1H, H5), 8.10−8.14 (m, 2H, H2′/H6′), 9.93 (br s, 1H, OH) ppm. ^{13}C{^{1}H} NMR (125.75 MHz, DMSO-d_6): δ = 114.6 (d, ^2J(C,F) = 24 Hz, C2′), 117.1 (d, ^2J(C,F) = 21 Hz, C4′), 119.0 (C8), 121.7 (C8a), 124.1 (d, ^4J(C,F) = 3 Hz, C6′), 125.2 (C7), 125.3 (C5), 131.1 (d, ^3J(C,F) = 8 Hz, C5′), 134.0 (d, ^3J(C,F) = 9 Hz, C1′), 134.4 (C6), 140.0 (C2), 144.0 (C3), 155.0 (C4a) 162.0 (d, ^1J(C,F) = 243 Hz, C3′), 173.6 (C4) ppm. Elemental Anal. Calcd for $C_{15}H_9FO_3$: C 70.31, H 3.54%. Found: C 69.94, H 3.39%.

*3-Hydroxy-2-(2-fluorophenyl)-chromen-4(1H)-one (**2e**).* The synthesis was performed according to the general procedure by using **1** (2.00 g, 14.7 mmol) and **e** (1.82 g, 14.7 mmol), affording **2e** as a yellow powder (0.87 g, 49%); mp 181−182 °C. ^{1}H NMR (500.10 MHz, DMSO-d_6): δ = 7.37−7.42 (m, 2H, H3′/H6′), 7.48−7.51 (m, 1H, H7), 7.59−7.63 (m, 1H, H4′), 7.66 (d, ^3J(H,H) = 8 Hz, 1H, H8), 7.76−7.82 (m, 2H, H5′/H6), 8.16 (dd, ^4J(H,H) = 1 Hz, ^3J(H,H) = 8 Hz, 1H, H5), 9.41 (br s, 1H, OH) ppm. ^{13}C{^{1}H} NMR (125.75 MHz, DMSO-d_6): δ = 116.6 (d, ^2J(C,F) = 21 Hz, C3′), 118.9 (C8), 119.5 (d, ^2J(C,F) = 14 Hz, C1′), 122.3 (C8a), 124.9 (d, ^3J(C,F) = 3 Hz, C6′), 125.2 (C7), 125.5 (C5), 131.7 (d, ^4J(C,F) = 2 Hz, C5′), 133.0 (d, ^3J(C,F) = 8 Hz, C4′), 134.3 (C6), 140.0 (C3), 143.9 (C2), 155.5 (C4a), 159.0 (d, ^1J(C,F) = 252 Hz, C2′), 173.2 (C4) ppm. Elemental Anal. Calcd for $C_{15}H_9FO_3$·0.05H_2O: C 70.31, H 3.54%. Found: C 69.98, H 3.42%.

*3-Hydroxy-2-(4-chlorophenyl)-chromen-4(1H)-one (**2f**).* The synthesis was performed according to the general procedure by using **1** (2.00 g, 14.7 mmol) and **f** (2.10 g, 14.7 mmo) to afford **2f** as yellow powder (2.31 g, 58%); mp 202−204 °C. ^{1}H NMR (500.10 MHz, DMSO-d_6): δ = 7.48−7.51 (m, 1H, H7), 7.65 (d, ^3J(H,H) = 8 Hz, 2H, H3′/H5′), 7.78 (d, ^3J(H,H) = 8 Hz, 1H, H8), 7.83−7.85 (m, 1H, H6), 8.13 (dd, ^4J(H,H) = 1 Hz, ^3J(H,H) = 8 Hz, 1H, H5), 8.26 (d, ^3J(H,H) = 9 Hz, 2H, H2′/H6′), 9.84 (br s, 1H, OH) ppm. ^{13}C{^{1}H} NMR (125.75 MHz, DMSO-d_6): δ = 118.9 (C8), 121.7 (C8a), 125.1 (C7), 125.3 (C5), 129.2 (C2′/C6′), 129.8 (C3′/C5′), 130.7 (C2), 134.4 (C6), 139.9 (C4′), 140.3 (C1′), 144.5 (C3), 155.0 (C4a), 173.5 (C4) ppm. Elemental Anal. Calcd for $C_{15}H_9ClO_3$: C 66.07, H 3.33%. Found: C 65.80, H 3.17%.

*3-Hydroxy-2-(3-chlorophenyl)-chromen-4(1H)-one (**2g**).* The synthesis was performed according to the general procedure by using **1** (2.00 g, 14.7 mmol) and **g** (2.10 g, 14.7 mmol), affording **2g** as a yellow powder (1.15 g, 29%); mp 157−159 °C. ^{1}H NMR (500.10 MHz, DMSO-d_6): δ = 7.48−7.51 (m, 1H, H4′), 7.58−7.64 (m, 2H, H5′/H7), 7.81−7.85 (m, 2H, H6/H8), 8.12 (d, ^3J(H,H) = 8 Hz, 1H, H5), 8.20 (d, ^3J(H,H) = 8 Hz, 1H, H6′), 8.28 (s, 1H, H2′), 9.93 (br s, 1H, OH) ppm. ^{13}C{^{1}H} NMR (125.75 MHz, DMSO-d_6): δ = 119.0 (C8), 121.7 (C8a), 125.2 (C7), 125.3 (C5), 126.7 (C6′), 127.5 (C2′), 130.1 (C4′), 131.0 (C5′), 133.8 (C2/C3′), 134.4 (C6), 140.1 (C1′), 143.9 (C3), 155.1 (C4a), 173.6 (C4) ppm. Elemental Anal. Calcd for $C_{15}H_9ClO_3$·0.1H_2O: C 65.64, H 3.38%. Found: C 65.69, H 3.19%.

*3-Hydroxy-2-(2-chlorophenyl)-chromen-4(1H)-one (**2h**).* The synthesis was performed according to the general procedure by using **1** (2.00 g, 14.7 mmol) and **h** (2.10 g, 14.7 mmol), affording **2h** as deep-yellow needles (2.69 g, 67%); mp 177−179 °C. ^{1}H NMR (500.10 MHz, DMSO-d_6): δ = 7.49−7.54 (m, 2H, H5′/H7), 7.57−7.61 (m, 1H, H3′), 7.66−7.68 (m, 2H, H4′/H8), 7.72 (dd, ^4J(H,H) = 2 Hz, ^3J(H,H) = 8 Hz, 1H, H6′), 7.80−7.83 (m, 1H, H6), 8.17 (dd, ^4J(H,H) = 1 Hz, ^3J(H,H) = 8 Hz, 1H, H5), 9.34 (br s, 1H, OH) ppm. ^{13}C{^{1}H} NMR (125.75 MHz, DMSO-d_6): δ = 118.9 (C8), 122.5 (C8a), 125.2 (C7), 125.5 (C5), 127.7 (C5′), 130.2 (C4′), 130.5 (C2′), 132.3 (C3′), 132.5 (C6′), 133.2 (C1′), 134.3 (C6), 139.7 (C2), 146.6 (C3), 155.5 (C4a), 173.4 (C4) ppm. Elemental Anal. Calcd for $C_{15}H_9ClO_3$·0.1H_2O: C 65.64, H 3.38%. Found: C 65.69, H 3.27%.

*3-Hydroxy-2-(4-bromophenyl)-chromen-4(1H)-one (**2i**).* The synthesis was performed according to the general procedure by using **1** (2.00 g, 14.7 mmol) and **I** (2.70 g, 14.7 mmol), affording **2i** as a yellow powder (2.31 g, 58%); mp 163−167 °C. ^{1}H NMR (500.10 MHz, DMSO-d_6): δ = 7.47−7.50 (m, 1H, H7), 7.77−7.87 (m, H3′/H5′/H6/H8), 8.12 (dd, ^4J(H,H) = 1 Hz, ^3J(H,H) = 8 Hz, 1H, H5), 8.19 (d, ^3J(H,H) = 9 Hz, 2H, H2′/H6′), 9.85 (br s, 1H, OH) ppm. ^{13}C{^{1}H} NMR (125.75 MHz, DMSO-d_6): δ = 118.9 (C8), 121.8 (C8a), 123.8 (C4′), 125.1 (C7), 125.3 (C5), 130.0 (C2), 132.1 (C3′/C5′), 134.4 (C6), 139.9 (C1′), 144.5 (C3), 155.0 (C4a), 173.5 (C4) ppm. Elemental Anal. Calcd for $C_{15}H_9BrO_3\cdot0.1H_2O$: C 56.49, H 2.91%. Found: C 56.51, H 2.68%.

*3-Hydroxy-2-(3-bromophenyl)-chromen-4(1H)-one (**2j**).* The synthesis was performed according to the general procedure by using **1** (2.00 g, 14.7 mmol) and **j** (2.70 g, 14.7 mmol), affording **2j** as orange crystals (0.82 g, 18%); mp 165−167 °C. ^{1}H NMR (500.10 MHz, DMSO-d_6): δ = 7.48−7.51 (m, 1H, H7), 7.56 (dd, ^3J(H,H) = 8 Hz, ^3J(H,H) = 8 Hz, 1H, H5′), 7.72−7.74 (m, 1H, H4′), 7.82−7.86 (m, 2H, H6/H8), 8.13 (dd, ^4J(H,H) = 1 Hz, ^3J(H,H) = 8 Hz, 1H, H5), 8.24−8.25 (m, 1H, H6′), 8.41−8.43 (m, 1H, H2′), 9.92 (br s, 1H, OH) ppm. ^{13}C{^{1}H} NMR (125.75 MHz, DMSO-d_6): δ = 119.0 (C8), 121.8 (C8a), 122.3 (C3′), 125.2 (C7), 125.3 (C5), 126.9 (C6′), 127.5 (C2′), 130.4 (C4′), 131.2 (C5′), 132.9 (C4′), 134.1 (C2), 134.4 (C6), 140.1 (C1′), 143.8 (C3), 155.1 (C4a), 173.6 (C4) ppm. Elemental Anal. Calcd for $C_{15}H_9BrO_3$: C 56.81, H 2.86%. Found: C 56.65, H 2.76%.

General Procedure for the Synthesis of the Ru^{II}(η^6-*p*-Cymene) Complexes 3a−3j. A solution of [Ru(η^6-*p*-cymene)Cl$_2$]$_2$ (0.45 equiv) in dichloromethane (15 mL) was added to a solution of 3-hydroxyflavones **2a**−**j** (1.00 equiv) and sodium methoxide (1.10 equiv) in methanol (15 mL). The reaction mixture was stirred at room temperature and under argon atmosphere for 18 h. The solvent was evaporated in vacuo, and the residue was extracted with dichloromethane, filtered, and concentrated. The pure product was obtained by recrystallization from methanol.

*[Chlorido{3-(oxo-κO)-2-phenyl-chromen-4(1H)-onato-κO}(η^6-*p*-cymene)ruthenium(II)] (**3a**).* The reaction was performed according to the general complexation procedure by using **2a** (164 mg, 0.73 mmol), NaOMe (43 mg, 0.8 mmol), and [Ru(η^6-*p*-cymene)Cl$_2$]$_2$ (200 mg, 0.33 mmol) affording **3a** as a deep-red powder (170 mg, 51%); mp 229−230 °C (decomp). ^{1}H NMR (500.10 MHz, CDCl$_3$): δ = 1.41−1.44 (m, 6H, CH$_{3,Cym}$), 2.43 (s, 3H, CH$_{3,Cym}$), 2.99−3.05 (m, 1H, CH$_{Cym}$), 5.39 (dd, ^3J(H,H) = 5 Hz, ^3J(H,H) = 5 Hz, 2H, H3/H5$_{Cym}$), 5.67 (dd, ^3J(H,H) = 5 Hz, ^3J(H,H) = 5 Hz, 2H, H2/H6$_{Cym}$), 7.33−7.35 (m, 1H, H7), 7.41 (dd, ^3J(H,H) = 7 Hz, ^3J(H,H) = 7 Hz, 1H, H4′), 7.48 (dd, ^3J(H,H) = 7 Hz, ^3J(H,H) = 7 Hz, 2H, H3′/H5′), 7.57 (d, ^3J(H,H) = 8 Hz, 1H, H8), 7.59−7.61 (m, 1H, H6), 8.22 (dd, ^4J(H,H) = 1 Hz, ^3J(H,H) = 8 Hz, 1H, H5), 8.61 (d, ^3J(H,H) = 7 Hz, 2H, H2′/H6′) ppm. ^{13}C{^{1}H} NMR (125.75 MHz, CDCl$_3$): δ = 18.7 (CH$_{3,Cym}$), 22.5 (CH$_{3,Cym}$), 31.3 (CH$_{Cym}$), 78.0 (C3/C5$_{Cym}$), 81.0 (C2/C6$_{Cym}$), 95.9 (C4$_{Cym}$), 98.9 (C1$_{Cym}$), 117.9 (C8), 120.0 (C8a), 124.0 (C7), 124.6 (C5), 127.3 (C2′/C6′), 128.2 (C3′/C5′), 129.3 (C4′), 132.5 (C2), 132.6 (C6), 149.2 (C1′), 153.9 (C4a), 154.0 (C3), 183.3 (C4) ppm. Elemental Anal. Calcd for $C_{25}H_{23}ClO_3Ru$: C 59.11, H 4.56%. Found: C 59.04, H 4.39%.

*[Chlorido{3-(oxo-κO)-2-(4-methylphenyl)-chromen-4(1H)-onato-κO}(η^6-*p*-cymene)ruthenium(II)] (**3b**).* The reaction was performed according to the general complexation procedure by using **2b** (184 mg, 0.73 mmol), NaOMe (43 mg, 0.8 mmol), and [Ru(η^6-*p*-cymene)Cl$_2$]$_2$ (200 mg, 0.33 mmol), affording **3b** as a red powder (240 mg, 68%). Single crystals suitable for X-ray diffraction analysis were grown from CHCl$_3$/*n*-hexane; mp 235−236 °C (decomp). ^{1}H NMR (500.10 MHz, CDCl$_3$): δ = 1.40−1.43 (m, 6H, CH$_{3,Cym}$), 2.42 (s, 3H, CH$_{3,Cym}$), 2.44 (s, 3H, CH$_3$), 2.98−3.04 (m, 1H, CH$_{Cym}$), 5.38 (dd, ^3J(H,H) = 5 Hz, ^3J(H,H) = 5 Hz, 2H, H3/H5$_{Cym}$), 5.65 (dd, ^3J(H,H) = 6 Hz, ^3J(H,H) = 6 Hz, 2H, H2/H6$_{Cym}$), 7.28 (d, ^3J(H,H) = 9 Hz, 2H, H3′/H5′), 7.32−7.35 (m, 1H, H7), 7.55 (d, ^3J(H,H) = 8 Hz, 1H, H8), 7.58−7.61 (m, 1H, H6), 8.21 (dd, ^4J(H,H) = 1 Hz, ^3J(H,H) = 8 Hz, 1H, H5), 8.50 (d, ^3J(H,H) = 8 Hz, 2H, H2′/H6′) ppm. ^{13}C{^{1}H} NMR (125.75 MHz, CDCl$_3$): δ = 18.7 (CH$_{3,Cym}$), 21.6 (CH$_3$), 22.5 (CH$_{3,Cym}$), 31.2 (CH$_{Cym}$), 77.9 (C3/C5$_{Cym}$), 80.9 (C2/C6$_{Cym}$), 95.9 (C4$_{Cym}$), 98.9 (C1$_{Cym}$), 117.8 (C8), 120.4 (C8a), 124.0 (C7), 124.5 (C5), 127.3 (C2′/C6′), 129.0 (C3′/C5′), 130.0 (C2), 132.6 (C6), 139.8 (C4′), 149.9 (C1′), 153.7 (C4a), 154.2 (C3), 183.1 (C4) ppm. Elemental Anal. Calcd for $C_{26}H_{25}ClO_3Ru$: C 59.82, H 4.83%. Found: C 59.82, H 4.57%.

*[Chlorido{3-(oxo-κO)-2-(4-fluorophenyl)-chromen-4(1H)-onato-κO}(η^6-*p*-cymene)ruthenium(II)] (**3c**).* The reaction was performed according to the general complexation procedure by using **2c** (187 mg, 0.73 mmol), NaOMe (43 mg, 0.8 mmol), and [Ru(η^6-*p*-cymene)Cl$_2$]$_2$ (200 mg, 0.33 mmol), affording **3c** as red needles (230 mg, 66%); mp 235−236 °C (decomp). ^{1}H NMR (500.10 MHz, CDCl$_3$): δ = 1.40−1.44 (m, 6H, CH$_{3,Cym}$), 2.42 (s, 3H, CH$_{3,Cym}$), 2.97−3.04 (m, 1H, CH$_{Cym}$), 5.40 (dd, ^3J(H,H) = 5 Hz, ^3J(H,H) = 5 Hz, 2H, H3/H5$_{Cym}$), 5.66 (dd, ^3J(H,H) = 5 Hz, ^3J(H,H) = 5 Hz, 2H, H2/H6$_{Cym}$), 7.15−7.18 (m, 2H, H3′/H5′), 7.33−7.36 (m, 1H, H7), 7.54 (d, ^3J(H,H) = 8 Hz, 1H, H8), 7.60−7.62 (m, 1H, H6), 8.22 (dd, ^4J(H,H) = 1 Hz, ^3J(H,H) = 8 Hz, 1H, H5), 8.61−8.64 (m, 2H, H2′/H6′) ppm. ^{13}C{^{1}H} NMR (125.75 MHz, CDCl$_3$): δ = 18.7 (CH$_{3,Cym}$), 22.5 (CH$_{3,Cym}$), 31.3 (CH$_{Cym}$), 78.0 (C3/C5$_{Cym}$), 81.0 (C2/C6$_{Cym}$), 95.9 (C4$_{Cym}$), 98.9 (C1$_{Cym}$), 115.2 (d, ^2J(C,F) = 21 Hz, C3′/C5′), 117.7 (C8), 120.1 (C8a), 124.1 (C7), 124.6 (C5), 128.8 (C2), 129.4 (d, ^3J(C,F) = 8 Hz, C2′/C6′), 132.6 (C6), 148.4 (d, ^4J(C,F) = 1 Hz, C1′), 153.8 (C4a), 154.1 (C3), 163.0 (d, ^1J(C,F) = 251 Hz, C4′), 183.3 (C4) ppm. Elemental Anal. Calcd for $C_{25}H_{22}ClFO_3Ru$: C 57.09, H 4.22%. Found: C 56.98, H 4.06%.

*[Chlorido{3-(oxo-κO)-2-(3-fluorophenyl)-chromen-4-onato-κO}(η^6-*p*-cymene)ruthenium(II)] (**3d**).* The reaction was performed according to the general complexation procedure by using **2d** (187 mg, 0.73 mmol), NaOMe (43 mg, 0.8 mmol), and [Ru(η^6-*p*-cymene)Cl$_2$]$_2$ (200 mg, 0.33 mmol), affording **3d** as deep-red powder (180 mg, 51%); mp 210−212 °C (decomp). Single crystals suitable for X-ray diffraction analysis were grown from CHCl$_3$/*n*-hexane. ^{1}H NMR (500.10 MHz, CDCl$_3$): δ = 1.40−1.46 (m, 6H, CH$_{3,Cym}$), 2.42 (s, 3H, CH$_{3,Cym}$), 2.99−3.06 (m, 1H, CH$_{Cym}$), 5.40 (d, ^3J(H,H) = 6 Hz, 2H, H3/H5$_{Cym}$), 5.68 (dd, ^3J(H,H) = 5 Hz, ^3J(H,H) = 5 Hz, 2H, H2/H6$_{Cym}$), 7.08 (ddd, ^4J(H,F) = 2 Hz, ^3J(H,H) = 8 Hz, ^3J(H,H) = 8 Hz, 1H, H4′), 7.33−7.36 (m, 1H, H7), 7.44 (ddd, ^3J(H,F) = 6 Hz, ^3J(H,H) = 8 Hz, ^3J(H,H) = 8 Hz, 1H, H5′), 7.56 (d, ^3J(H,H) = 8 Hz, 1H, H8), 7.61−7.65 (m, 1H, H6), 8.22 (dd, ^4J(H,H) = 1 Hz, ^3J(H,H) = 8 Hz, 1H, H5), 8.31 (d, ^3J(H,H) = 8 Hz, 1H, H6′), 8.44−8.48 (m, 1H, H2′) ppm. ^{13}C{^{1}H} NMR (125.75 MHz, CDCl$_3$): δ = 18.7 (CH$_{3,Cym}$), 22.5 (2CH$_{3,Cym}$), 31.3 (CH$_{Cym}$), 78.0 (C3/C5$_{Cym}$), 80.0 (C2/C6$_{Cym}$), 95.9 (C4$_{Cym}$), 99.0 (C1$_{Cym}$), 114.1 (d, ^2J(C,F) = 25 Hz, C2′), 115.8 (d, ^2J(C,F) = 22 Hz, C4′), 117.9 (C8), 119.9 (C8a), 122.5 (d, ^4J(C,F) = 3 Hz, C6′), 124.2 (C7), 124.7 (C5), 127.2 (C2), 129.6 (d, ^3J(C,F) = 8 Hz, C5′), 132.9 (C6), 125.5 (d, ^3J(C,F) = 9 Hz, C1′), 153.9 (C4a), 154.9 (C3), 162.0 (d, ^1J(C,F) = 243 Hz, C3′), 183.8 (C4) ppm. Elemental Analysis Calcd for $C_{25}H_{22}ClFO_3Ru\cdot0.25H_2O$: C 56.61, H 4.28%. Found: C 56.51, H 4.28%.

*[Chlorido{3-(oxo-κO)-2-(2-fluorophenyl)-chromen-4-onato-κO}(η^6-*p*-cymene)ruthenium(II)] (**3e**).* The reaction was performed according to the general complexation procedure, by using **2e** (187 mg, 0.73 mmol), NaOMe (43 mg, 0.8 mmol), and [Ru(η^6-*p*-cymene)Cl$_2$]$_2$ (200 mg, 0.33 mmol), affording **3e** as red−brownish powder (220 mg, 63%); mp 199−202 °C (decomp). ^{1}H NMR (500.10 MHz, CDCl$_3$):): δ = 1.37−1.42 (m, 6H, CH$_{3,Cym}$), 2.39 (s, 3H, CH$_{3,Cym}$), 2.97−3.02 (m, 1H, CH$_{Cym}$), 5.36 (dd, ^3J(H,H) = 6 Hz, ^3J(H,H) = 6 Hz, 2H, H3/H5$_{Cym}$), 5.68 (d, ^3J(H,H) = 6 Hz, 2H, H2/H6$_{Cym}$), 7.14−7.19 (m, 1H, H3′), 7.21 (ddd, ^4J(H,F) = 1 Hz, ^3J(H,H) = 8 Hz, ^3J(H,H) = 8 Hz, 1H, H6′), 7.33−7.36 (m, 1H, H7), 7.38−7.42 (m, 1H, H4′), 7.51 (d, ^3J(H,H) = 8 Hz, 1H, H8), 7.58−7.62 (m, 1H, H6), 8.23 (dd, ^4J(H,H) = 1 Hz, ^3J(H,H) = 8 Hz, 1H, H5), 8.31 (ddd, ^4J(H,F) = 1 Hz, ^3J(H,H) = 7 Hz, ^3J(H,H) = 7 Hz, 1H, H5′) ppm. ^{13}C{^{1}H} NMR (125.75 MHz, CDCl$_3$): δ = 18.7 (CH$_{3,Cym}$), 22.5 (2CH$_{3,Cym}$), 31.2 (CH$_{Cym}$), 77.7 (C3/C5$_{Cym}$), 81.2 (C2/C6$_{Cym}$), 96.0 (C4$_{cym}$), 98.9 (C1$_{Cym}$), 116.3 (d, ^2J(C,F) = 22 Hz, C3′), 118.3 (C8), 120.1 (d, ^2J(C,F) = 10 Hz, C1′), 120.1 (C8a), 123.6 (d, ^3J(C,F) = 3 Hz, C6′), 124.1 (C7), 124.6 (C5), 131.1 (d, ^3J(C,F) = 8 Hz, C4′),

131.6 (d, ^4J(C,F) = 2 Hz, C5′), 132.7 (C6), 146.9 (C2/C3), 154.4 (C4a), 159.0 (d, ^1J(C,F) = 256 Hz, C2′), 183.6 (C4) ppm. Elemental Anal. Calcd for $C_{25}H_{22}ClFO_3Ru\cdot0.5H_2O$: C 56.13, H 4.33%. Found: C 56.22, H 4.60%.

*[Chlorido{3-(oxo-κO)-2-(4-chlorophenyl)-chromen-4(1H)-onato-κO}(η⁶-p-cymene)ruthenium(II)] (**3f**).* The reaction was performed according to the general complexation procedure by using **2f** (199 mg, 0.73 mmol), NaOMe (43 mg, 0.8 mmol), and $[Ru(\eta^6\text{-}p\text{-cymene})Cl_2]_2$ (200 mg, 0.33 mmol), affording **3f** as deep-red powder (226 mg, 63%); mp 214−217 °C (decomp). ^{1}H NMR (500.10 MHz, $CDCl_3$): δ = 1.32−1.38 (m, 6H, $CH_{3,Cym}$), 2.42 (s, 3H, $CH_{3,Cym}$), 2.85−2.91 (m, 1H, CH_{Cym}), 5.39 (dd, ^3J(H,H) = 5 Hz, ^3J(H,H) = 5 Hz, 2H, H3/H5$_{Cym}$), 5.66 (dd, ^3J(H,H) = 5 Hz, ^3J(H,H) = 5 Hz, 2H, H2/H6$_{Cym}$), 7.32−7.35 (m, 1H, H7), 7.44 (d, ^3J(H,H) = 9 Hz, 2H, H3′/H5′), 7.54 (d, ^3J(H,H) = 8 Hz, 1H, H8), 7.62−7.63 (m, 1H, H6), 8.21 (dd, ^4J(H,H) = 1 Hz, ^3J(H,H) = 8 Hz, 1H, H5), 8.55 (d, ^3J(H,H) = 9 Hz, 2H, H2′/H6′) ppm. ^{13}C{^{1}H} NMR (125.75 MHz, $CDCl_3$): δ = 18.7 ($CH_{3,Cym}$), 22.4 ($CH_{3,Cym}$), 30.0 (CH_{Cym}), 77.9 (C3/C5$_{Cym}$), 81.0 (C2/C6$_{Cym}$), 95.9 (C4$_{Cym}$), 99.0 (C1$_{Cym}$), 117.8 (C8), 120.0 (C8a), 124.1 (C7), 124.7 (C5), 125.5 (C2′/C6′/C3′/C5′), 131.0 (C2), 132.8 (C6), 134.9 (C4′), 143.5 (C1′), 153.9 (C4a), 154.6 (C3), 183.5 (C4). Elemental Anal. Calcd for $C_{25}H_{22}Cl_2O_3Ru$: C 55.36, H 4.09%. Found: C 55.28, H 3.90%.

*[Chlorido{3-(oxo-κO)-2-(3-chlorophenyl)-chromen-4-onato-κO}(η⁶-p-cymene)ruthenium(II)] (**3g**).* The reaction was performed according to the general complexation procedure by using **2g** (199 mg, 0.73 mmol), NaOMe (43 mg, 0.8 mmol), and $[Ru(\eta^6\text{-}p\text{-cymene})Cl_2]_2$ (200 mg, 0.33 mmol), affording **3g** as deep-red powder (244 mg, 68%); mp 213−220 °C (decomp). ^{1}H NMR (500.10 MHz, $CDCl_3$): δ = 1.43−1.48 (m, 6H, $CH_{3,Cym}$), 2.44 (s, 3H, $CH_{3,Cym}$), 3.00−3.07 (m, 1H, CH_{Cym}), 5.39 (dd, ^3J(H,H) = 5 Hz, ^3J(H,H) = 5 Hz, 2H, H3/H5$_{Cym}$), 5.68 (dd, ^3J(H,H) = 5 Hz, ^3J(H,H) = 5 Hz, 2H, H2/H6$_{Cym}$), 7.33−7.36 (m, 2H, H4′/H7), 7.40 (dd, ^3J(H,H) = 8 Hz, ^3J(H,H) = 8 Hz, 1H, H5′), 7.55 (d, ^3J(H,H) = 8 Hz, 1H, H8), 7.63−7.65 (m, 1H, H6), 8.21 (dd, ^4J(H,H) = 1 Hz, ^3J(H,H) = 8 Hz, 1H, H5), 8.41 (ddd, ^4J(H,H) = 1 Hz, ^3J(H,H) = 8 Hz, ^3J(H,H) = 8 Hz, 1H, H6′), 8.72−8.73 (m, 1H, H2′) ppm. ^{13}C{^{1}H} NMR (125.75 MHz, $CDCl_3$): δ = 18.7 ($CH_{3,Cym}$), 22.5 (2$CH_{3,Cym}$), 31.3 (CH_{Cym}), 77.9 (C3/C5$_{Cym}$), 81.2 (C2/C6$_{Cym}$), 95.8 (C4$_{Cym}$), 98.9 (C1$_{Cym}$), 117.9 (C8), 119.9 (C8a), 124.2 (C7), 124.7 (C5), 124.8 (C6′), 127.1 (C2′), 128.9 (C4′), 129.4 (C5′), 133.0 (C6), 134.2 (C2/C3′), 147.3 (C1′), 154.0 (C4a), 154.9 (C3), 183.8 (C4) ppm. Elemental Anal. Calcd for $C_{25}H_{22}Cl_2O_3Ru\cdot0.15H_2O$: C 55.08, H 4.12%. Found: C 55.11, H 3.85%.

*[Chlorido{3-(oxo-κO)-2-(2-chlorophenyl)-chromen-4-onato-κO}(η⁶-p-cymene)ruthenium(II)] (**3h**).* The reaction was performed according to the general complexation procedure by using **2h** (199 mg, 0.73 mmol), NaOMe (43 mg, 0.8 mmol), and $[Ru(\eta^6\text{-}p\text{-cymene})Cl_2]_2$ (200 mg, 0.33 mmol), affording **3h** as brown powder (109 mg, 30%); mp 205−208 °C (decomp). Single crystals suitable for X-ray diffraction analysis were grown from MeOH/*n*-hexane. ^{1}H NMR (500.10 MHz, $CDCl_3$): δ = 1.35−1.39 (m, 6H, $CH_{3,Cym}$), 2.37 (s, 3H, $CH_{3,Cym}$), 2.93−3.00 (m, 1H, CH_{Cym}), 5.35 (dd, ^3J(H,H) = 5 Hz, ^3J(H,H) = 5 Hz, 2H, H3/H5$_{Cym}$), 5.63 (dd, ^3J(H,H) = 5 Hz, ^3J(H,H) = 5 Hz, 2H, H2/H6$_{Cym}$), 7.34−7.38 (m, 3H, H3′/H5′/H7), 7.48−7.52 (m, 2H, H4′/H8), 7.60−7.62 (m, 1H, H6), 7.99−8.02 (m, 1H, H6′), 8.24 (dd, ^4J(H,H) = 1 Hz, ^3J(H,H) = 8 Hz, 1H, H5) ppm. ^{13}C{^{1}H} NMR (125.75 MHz, $CDCl_3$): δ = 18.9 ($CH_{3,Cym}$), 22.3 (2$CH_{3,Cym}$), 31.2 (CH_{Cym}), 77.5 (C3/C5$_{Cym}$), 80.5 (C2/C6$_{Cym}$), 96.1 (C4$_{Cym}$), 98.9 (C1$_{Cym}$), 118.2 (C8), 120.2 (C8a), 124.1 (C7), 124.6 (C5), 126.3 (C5′), 130.3 (C4′), 130.5 (C3′), 130.7 (C2′), 132.7 (C6′), 132.8 (C6), 133.4 (C1′), 148.5 (C2), 154.3 (C3), 154.5 (C4a), 184.1 (C4) ppm. Elemental Anal. Calcd for $C_{25}H_{22}Cl_2O_3Ru$: C 55.36, H 4.09%. Found: C 55.29, H 3.79%.

*[Chlorido{3-(oxo-κO)-2-(4-bromophenyl)-chromen-4-onato-κO}(η⁶-p-cymene)ruthenium(II) (**3i**).* The reaction was performed according to the general complexation procedure, by using **2i** (231 mg, 0.73 mmol), NaOMe (43 mg, 0.8 mmol), and $[Ru(\eta^6\text{-}p\text{-cymene})Cl_2]_2$ (200 mg, 0.33 mmol), affording **3i** as red powder (179 mg, 46%); mp 228−233 °C (decomp). ^{1}H NMR (500.10 MHz, $CDCl_3$): δ = 1.40−1.45 (m, 6H, $CH_{3,Cym}$), 2.42 (s, 3H, $CH_{3,Cym}$), 2.98−3.04 (m, 1H, CH_{Cym}), 5.39 (dd, ^3J(H,H) = 5 Hz, ^3J(H,H) = 5 Hz, 2H, H3/H5$_{Cym}$), 5.66 (dd, ^3J(H,H) = 5 Hz, ^3J(H,H) = 5 Hz, 2H, H2/H6$_{Cym}$), 7.33−7.36 (m, 1H, H7), 7.54 (d, ^3J(H,H) = 8 Hz, 1H, H8), 7.59−7.64 (m, 3H, H3′/H5′/H6), 8.21 (dd, ^4J(H,H) = 1 Hz, ^3J(H,H) = 8 Hz, 1H, H5), 8.48 (d, ^3J(H,H) = 9 Hz, 2H, H2′/H6′) ppm. ^{13}C{^{1}H} NMR (125.75 MHz, $CDCl_3$): δ = 18.7 ($CH_{3,Cym}$), 22.5 ($CH_{3,Cym}$), 31.3 (CH_{Cym}), 77.9 (C3/C5$_{Cym}$), 80.0 (C2/C6$_{Cym}$), 96.0 (C4$_{Cym}$), 99.0 (C1$_{Cym}$), 117.8 (C8), 120.0 (C8a), 123.4 (C4′), 124.1 (C7), 124.7 (C5), 128.6 (C2′/C6′), 131.4 (C3′/C5′), 131.7 (C2), 132.8 (C6), 148.0 (C1′), 153.9 (C4a), 154.7 (C3), 183.5 (C4) ppm. Elemental Anal. Calcd for $C_{25}H_{22}BrClO_3Ru\cdot0.25H_2O$: C 50.77, H 3.83%. Found: C 50.74, H 3.57%.

*[Chlorido{3-(oxo-κO)-2-(3-bromophenyl)-chromen-4-onato-κO}(η⁶-p-cymene)ruthenium(II)] (**3j**).* The reaction was performed according to the general complexation procedure by using **2j** (231 mg, 0.73 mmol), NaOMe (43 mg, 0.8 mmol), and $[Ru(\eta^6\text{-}p\text{-cymene})Cl_2]_2$ (200 mg, 0.33 mmol), affording **3j** as dark-brown crystals (153 mg, 40%); mp 213-219 °C (decomp). ^{1}H NMR (500.10 MHz, $CDCl_3$): δ = 1.44−1.49 (m, 6H, $CH_{3,Cym}$), 2.44 (s, 3H, $CH_{3,Cym}$), 3.00−3.07 (m, 1H, CH_{Cym}), 5.39 (dd, ^3J(H,H) = 5 Hz, ^3J(H,H) = 5 Hz, 2H, H3/H5$_{Cym}$), 5.68 (d, ^3J(H,H) = 5 Hz, ^3J(H,H) = 5 Hz, 2H, H2/H6$_{Cym}$), 7.33−7.36 (m, 2H, H5′/H7), 7.40 (ddd, ^4J(H,H) = 1 Hz, ^4J(H,H) = 2 Hz, ^3J(H,H) = 8 Hz, 1H, H4′), 7.56 (d, ^3J(H,H) = 8 Hz, 1H, H8), 7.62−7.65 (m, 1H, H6), 8.21 (dd, ^4J(H,H) = 1 Hz, ^3J(H,H) = 8 Hz, 1H, H5), 8.45−8.47 (m, 1H, H6′), 8.87−8.89 (m, 1H, H2′) ppm. ^{13}C{^{1}H} NMR (125.75 MHz, $CDCl_3$): δ = 18.7 ($CH_{3,Cym}$), 22.7 (2$CH_{3,Cym}$), 31.3 (CH_{Cym}), 77.9 (C3/C5$_{Cym}$), 81.2 (C2/C6$_{Cym}$), 95.7 (C4$_{Cym}$), 98.8 (C1$_{Cym}$), 117.9 (C8), 119.8 (C8a), 122.4 (C3′), 124.2 (C7), 124.8 (C5), 125.3 (C6′), 129.7 (C2′), 129.9 (C5′), 131.8 (C4′), 133.0 (C6), 134.5 (C2), 147.1 (C1′), 154.0 (C4a), 154.9 (C3), 183.8 (C4) ppm. Elemental Anal. Calcd for $C_{25}H_{22}BrClO_3Ru\cdot0.25H_2O$: C 49.64, H 4.00%. Found: C 49.40, H 3.85%.

Hydrolysis and Interaction with 5′-GMP. Hydrolysis and stability in water were investigated by ^{1}H NMR spectroscopy. Because of the lipophilic character of the organometallics, all experiments were performed in 10% DMSO-d_6/D_2O solutions. For the 5′-GMP binding studies, the complexes (ca. 0.1 mg/mL) were dissolved in 10% DMSO-d_6/D_2O, yielding the corresponding highly reactive aqua species. The aqua complexes were converted in situ by addition of 50 μL increments of 5′-GMP solution (10 mg/mL) into the respective 5′-GMP adduct, and the reaction was monitored by ^{1}H NMR spectroscopy until unconverted 5′-GMP was observed.

Cytotoxicity in Cancer Cell Lines. *Cell Lines and Culture Conditions.* CH1 cells originate from an ascites sample of a patient with a papillary cystadenocarcinoma of the ovary and were a gift from Lloyd R. Kelland, CRC Centre for Cancer Therapeutics, Institute of Cancer Research, Sutton, UK. SW480 (human adenocarcinoma of the colon) and A549 (human non-small cell lung cancer) cells were provided by Brigitte Marian (Institute of Cancer Research, Department of Medicine I, Medical University of Vienna, Austria). The cell lines 5637 (bladder cancer), LCLC-103H (lung cancer), and DAN-G (pancreatic cancer) were obtained from the German Collection of Microorganisms and Cell Culture (DSMZ, Braunschweig, FRG). Cells were grown in 75 cm^2 culture flasks (Iwaki) as adherent monolayer cultures in either Minimum Essential Medium (MEM) supplemented with 10% heat inactivated fetal calf serum (FCS), 1 mM sodium pyruvate, 4 mM L-glutamine, and 1% nonessential amino acids (from 100× stock) (i.e., CH1, SW480, and A549) or in RPMI 1640 medium supplemented with 10% FCS (i.e., 5637, LCLC-103H, DAN-G). All cell culture reagents were obtained from Sigma-Aldrich. Cultures were maintained at 37 °C in a humidified atmosphere containing 95% air and 5% CO_2.

MTT Assay. Cytotoxicity was determined by the colorimetric MTT [3-(4,5-dimethyl-2-thiazolyl)-2,5-diphenyl-2*H*-tetrazolium bromide, Fluka] microculture assay. For this purpose, cells were harvested from culture flasks by trypsinization and seeded in 100 μL aliquots into 96-well microculture plates (Iwaki). Cell densities of 1.5 × 10^3 cells/well (CH1), 2.5 × 10^3 cells/well (SW480), and 4 × 10^3 cells/well (A549) were chosen in order to ensure exponential growth of

untreated controls throughout the experiment. Cells were allowed to settle and resume exponential growth in drug-free complete culture medium for 24 h. Stock solutions of the test compounds in DMSO were appropriately diluted in complete culture medium so that the maximum DMSO content did not exceed 1%. These dilutions were added in 100 μL aliquots to the microcultures, and cells were exposed to the test compounds for 96 h. In case of the studies on time-dependent cytotoxicity, SW480 cells were treated for 1, 4, 24, and 96 h with **3j** followed by incubation in drug-free medium for the rest of a total incubation time of 96 h. At the end of incubation, all media were replaced by 100 μL/well RPMI1640 culture medium (supplemented with 10% heat-inactivated FCS) plus 20 μL/well MTT solution in phosphate-buffered saline (5 mg/mL). After incubation for 4 h, the supernatants were removed and the formazan crystals formed by viable cells were dissolved in 150 μL of DMSO per well. Optical densities at λ = 550 nm were measured with a microplate reader (Tecan Spectra Classic) by using a reference wavelength of 690 nm to correct for unspecific absorption. The quantity of viable cells was expressed in terms of T/C values by comparison to untreated controls, and 50% inhibitory concentrations (IC_{50}) were calculated from concentration−effect curves by interpolation. Evaluation is based on means from at least three independent experiments, each comprising at least three replicates per concentration level.

Crystal Violet Assay Conditions. This assay has been described in detail elsewhere.[49] Culture conditions were the same as used in the MTT assay. Briefly, cells were seeded into 96-well microculture plates (Sarstedt, FRG) in cell densities of 1.0×10^3 cells/well, except for LCLC-103H, which was seeded at 250 cells/well. After a 24 h preincubation, cells were treated with the test substance for 96 h. Stock solutions of the test substance were prepared to 20 mM in DMF and diluted 1000-fold in RPMI 1640 culture medium containing 10% FCS. Substances that showed a ≥50% growth inhibition at 20 μM were tested at five serial dilutions in four wells/concentration to determine the IC_{50} values as described.[49] The staining of the cells was done for 30 min with a 0.02% crystal violet solution in water followed by washing out the excess dye. Cell bound dye was redissolved in 70% ethanol/water solution, and the optical densities at λ = 570 nm were measured with a microplate reader (Anthos 2010).

Cell Cycle Analysis. One million A549 cells were seeded into Petri dishes and allowed to recover for 24 h. Cells were then exposed for 48 h to the test compounds. Control and drug-treated cells were collected, washed with PBS, fixed in 70% ice-cold ethanol, and stored at −20 °C. To determine cell cycle distribution, cells were transferred in physiological NaCl solution into PBS, incubated with 10 μg/mL RNase A for 30 min at 37 °C, followed by 30 min treatment with 5 μg/mL propidium iodide. Fluorescence was measured by flow cytometry by using FACS Calibur (Becton Dickinson, Palo Alto, CA). The resulting DNA histograms were quantified by Cell Quest Pro software (Becton Dickinson and Company, New York, USA).

Determination of Topoisomerase IIα Activity. Effects on the catalytic activity of topoisomerase IIα were determined using a decatenation assay. Catenated kinetoplast DNA (kDNA) was used as a substrate. kDNA is an aggregate of interlocked DNA minicircles (mostly 2.5 kb), which can be released by topoisomerase IIα. kDNA (200 ng, TopoGen, OH, USA) was incubated in a final volume of 30 μL (containing 40 ng of topoisomerase IIα; 50 mM Tris, pH 7.9; 120 mM KCl; 10 mM $MgCl_2$; 1 mM ATP; 0.5 mM DTT; 0.5 mM EDTA; 0.03 mg/mL BSA) at 37 °C for 60 min. The reaction was stopped by the addition of 1/10 volume of 1 mg/mL proteinase K in 10% (w/v) SDS and incubation at 37 °C for further 30 min. Gel electrophoresis was performed in the absence of ethidium bromide at 60 V for 3 h in 1% (w/v) agarose gels with Tris acetate/EDTA buffer (40 mM Tris; 1 mM EDTA, pH 8.5; 20 mM acetic acid). Subsequently, the gel was stained in 10 μg/mL ethidium bromide solution for 20 min. The fluorescence of ethidium bromide was detected with the LAS-4000 system (Fujifilm, Raytest, Germany).

CDK2/Cyclin A Protein Kinase Inhibition Assay. The CDK2 peptide substrate, HHASPRK, and the CDK2/Cyclin A protein complex were purchased from Enzo Life Sciences. Adenosine 5′-[γ-ferrocene] triphosphate (Fc-ATP) was synthesized according to the procedure published elsewhere.[35] Gold disk electrodes (99.99% purity) with surface area of 0.02 cm^2 were obtained from CHInstruments. All experiments were conducted in aqueous conditions using ultrapure water (18.2 MΩ cm) from a Millipore Milli-Q system.

Fabrication of Kinase Biosensor. The gold electrodes were cleaned by polishing with slurry of 1 μm Al_2O_3 until a mirror finish was obtained. After 5 min sonication in Milli-Q water, the gold electrodes were rinsed with water and ethanol. The electrodes were then cleaned electrochemically by cyclic voltammetry (CV) in the negative potential range from −0.6 to −2.3 V in 0.5 M KOH, followed by cycling in 0.5 M H_2SO_4 in the 0−1.2 V potential range. Next, the gold electrodes were incubated with 2 mM lipoic acid *N*-hydroxysuccinimide ester solution in ethanol for 3 days at 273 K. After extensive washing with freshly distilled ethanol, the gold electrodes were incubated with a 0.1 mM peptide solution in Milli-Q water for 18 h at 273 K. Consequently, the modified electrodes were rinsed with Milli-Q water and then incubated with 100 mM ethanolamine solution in absolute ethanol for 1 h. Finally, the electrodes were immersed in 10 mM dodecanethiol solution in ethanol for 20 min to block any unmodified gold surface.

Kinase-Catalyzed Fc-Phosphorylation Reaction. The peptide-modified gold electrodes were immersed in the kinase assay buffer based on 60 mM HEPES (pH 7.5), 3 mM $MnCl_2$, 3 mM $MgCl_2$, 0.5 μg/μL of PEG 20000, 3 μM sodium *ortho*-vanadate, 1 μg/mL CDK2/cyclin A protein kinase and 200 μM Fc-ATP. The phosphorylation reaction was performed for 6 h at 37 °C in a heating block (VWR Scientific, USA). The modified gold electrodes were washed five times using the kinase assay buffer and 0.1 M phosphate buffer (pH 7.4) prior to the electrochemical measurement. For the inhibitor studies, the CDK2/cyclin A protein and compounds **3a**−**h** (1 mM, DMSO) were added to the kinase buffer while maintaining the working concentration of the protein and inhibitor at 1 μg/mL and 10 μM, respectively. The DMSO concentration was maintained at a low level (<2%). After 30 min, the kinase reaction was initiated by the addition of Fc-ATP and was followed by the procedure outlined above.

Electrochemical Experiments. All electrochemical experiments were carried out using a CHInstrument 660B system potentiostat (Austin, TX) at a 100 mV/s scan rate unless otherwise specified. The electrochemical measurements were performed in 0.1 M phosphate buffer (pH 7.4). Typical electrochemical experimental set up included a three-electrode system: a modified gold electrode as the working electrode, Ag/AgCl in 3 M KCl as the reference electrode, which was connected with the electrolyte via a salt bridge, and platinum wire as the counter electrode. For each electrode, cyclic voltammetry was performed at a scan rate of 100 mV/s and square-wave voltammetry was recorded from 0.2 to 0.6 V, with an amplitude of 25 mV at 20 Hz frequency.

■ ASSOCIATED CONTENT

Ⓢ Supporting Information

Single crystal X-ray diffraction data for compounds **3d**, **3f**, and **3h**, NMR spectra demonstrating the stability of **3i** over two years and the binding ability of **3a** to the DNA model 5′-GMP, concentration−effect curves for different cell lines, the cell cycle distribution in dependence of the concentration of Ru complex, data on the topoisomerase IIα inhibitory activity, and electrochemical data. This material is available free of charge via the Internet at http://pubs.acs.org.

■ AUTHOR INFORMATION

Corresponding Author

*Phone: +64 9 373 7599 ext 83220. Fax: +64 9 373 7599 87422. E-mail: c.hartinger@auckland.ac.nz. Web site: http://hartinger.wordpress.fos.auckland.ac.nz/. Address: The University of Auckland, School of Chemical Sciences, Private Bag 92019, Auckland 1142, New Zealand.

Notes

The authors declare no competing financial interest.

■ ACKNOWLEDGMENTS

We thank the University of Vienna, the Austrian Science Fund (FWF), the Johanna Mahlke geb. Obermann Foundation, and COST D39 for financial support. We gratefully acknowledge Alexander Roller for collecting the X-ray diffraction data. V. Dirsch and D. Schachner (Department of Pharmacognosy, University of Vienna) are gratefully acknowledged for providing the FACS instrument and for technical instructions, respectively.

■ ABBREVIATIONS USED

5′-GMP, guanosine 5′-monophosphate; CDK, cyclin dependent kinase; CV, cyclic voltammetry; cym, η^6-*p*-cymene; Fc-ATP, adenosine 5′-[γ-ferrocene] triphosphate; IC_{50}, 50% inhibitory concentration; kDNA, kinetoplast DNA; pta, 1,3,5-triaza-7-phoshatricyclo-[3.3.1.1]decane; SWV, square-wave voltammetry

■ REFERENCES

(1) Jakupec, M. A.; Galanski, M.; Arion, V. B.; Hartinger, C. G.; Keppler, B. K. Antitumor metal compounds: more than theme and variations. *Dalton Trans.* **2008**, 183−194.

(2) Heffeter, P.; Jungwirth, U.; Jakupec, M.; Hartinger, C.; Galanski, M.; Elbling, L.; Micksche, M.; Keppler, B.; Berger, W. Resistance against novel anticancer metal compounds: differences and similarities. *Drug Resist. Updates* **2008**, *11*, 1−16.

(3) Clarke, M. J. Ruthenium metallopharmaceuticals. *Coord. Chem. Rev.* **2003**, *236*, 209−233.

(4) Hartinger, C. G.; Jakupec, M. A.; Zorbas-Seifried, S.; Groessl, M.; Egger, A.; Berger, W.; Zorbas, H.; Dyson, P. J.; Keppler, B. K. KP1019, a new redox-active anticancer agent—preclinical development and results of a clinical phase I study in tumor patients. *Chem. Biodiversity* **2008**, *5*, 2140−2155.

(5) Hartinger, C. G.; Zorbas-Seifried, S.; Jakupec, M. A.; Kynast, B.; Zorbas, H.; Keppler, B. K. From bench to bedside—preclinical and early clinical development of the anticancer agent indazolium *trans*-[tetrachlorobis(1*H*-indazole)ruthenate(III)] (KP1019 or FFC14A). *J. Inorg. Biochem.* **2006**, *100*, 891−904.

(6) Rademaker-Lakhai, J. M.; Van Den Bongard, D.; Pluim, D.; Beijnen, J. H.; Schellens, J. H. M. A phase I and pharmacological study with imidazolium-*trans*-DMSO-imidazole-tetrachlororuthenate, a novel ruthenium anticancer agent. *Clin. Cancer Res.* **2004**, *10*, 3717−3727.

(7) Ang, W. H.; Casini, A.; Sava, G.; Dyson, P. J. Organometallic ruthenium-based antitumor compounds with novel modes of action. *J. Organomet. Chem.* **2011**, *696*, 989−998.

(8) Hartinger, C. G.; Dyson, P. J. Bioorganometallic chemistry—from teaching paradigms to medicinal application. *Chem. Soc. Rev.* **2009**, *38*, 391−401.

(9) Zimmermann, G. R.; Lehár, J.; Keith, C. T. Multi-target therapeutics: when the whole is greater than the sum of the parts. *Drug Discovery Today* **2007**, *12*, 34−42.

(10) Kurzwernhart, A.; Kandioller, W.; Bartel, C.; Bächler, S.; Trondl, R.; Mühlgassner, G.; Jakupec, M. A.; Arion, V. B.; Marko, D.; Keppler, B. K.; Hartinger, C. G. Targeting the DNA−topoisomerase complex in a double-strike approach with a topoisomerase inhibiting moiety and covalent DNA binder. *Chem. Commun.* **2012**, *48*, 4839−4841.

(11) Cushnie, T. P. T.; Lamb, A. J. Antimicrobial activity of flavonoids. *Int. J. Antimicrob. Agents* **2005**, *26*, 343−356.

(12) Harborne, J. B.; Williams, C. A. Advances in flavonoid research since 1992. *Phytochemistry* **2000**, *55*, 481−504.

(13) Middleton, E., Jr.; Kandaswami, C.; Theoharides, T. C. The effects of plant flavonoids on mammalian cells: implications for inflammation, heart disease, and cancer. *Pharmacol. Rev.* **2000**, *52*, 673−751.

(14) Sathish, S.; Narayan, G.; Rao, N.; Janardhana, C. A self-organized ensemble of fluorescent 3-hydroxyflavone−Al(III) complex as sensor for fluoride and acetate ions. *J. Fluoresc.* **2007**, *17*, 1−5.

(15) Mladěnka, P.; Macáková, K.; Filipský, T.; Zatloukalová, L.; Jahodář, L.; Bovicelli, P.; Silvestri, I. P.; Hrdina, R.; Saso, L. In vitro analysis of iron chelating activity of flavonoids. *J. Inorg. Biochem.* **2011**, *105*, 693−701.

(16) Roshal, A. D.; Grigorovich, A. V.; Doroshenko, A. O.; Pivovarenko, V. G.; Demchenko, A. P. Flavonols as metal-ion chelators: complex formation with Mg^{2+} and Ba^{2+} cations in the excited state. *J. Photochem. Photobiol., A* **1999**, *127*, 89−100.

(17) Grazul, M.; Budzisz, E. Biological activity of metal ions complexes of chromones, coumarins and flavones. *Coord. Chem. Rev.* **2009**, *253*, 2588−2598.

(18) Bennett, M.; Burke, A. J.; O'Sullivan, W. I. Aspects of the Algar−Flynn−Oyamada (AFO) reaction. *Tetrahedron* **1996**, *52*, 7163−7178.

(19) Geissman, T. A.; Fukushima, D. K. Flavanones and related compounds. V. The oxidation of 2′-hydroxychalcones with alkaline hydrogen peroxide. *J. Am. Chem. Soc.* **1948**, *70*, 1686−1689.

(20) Qin, C. X.; Chen, X.; Hughes, R. A.; Williams, S. J.; Woodman, O. L. Understanding the cardioprotective effects of flavonols: discovery of relaxant flavonols without antioxidant activity. *J. Med. Chem.* **2008**, *51*, 1874−1884.

(21) Kandioller, W.; Hartinger, C. G.; Nazarov, A. A.; Kasser, J.; John, R.; Jakupec, M. A.; Arion, V. B.; Dyson, P. J.; Keppler, B. K. Tuning the anticancer activity of maltol-derived ruthenium complexes by derivatization of the 3-hydroxy-4-pyrone moiety. *J. Organomet. Chem.* **2009**, *694*, 922−929.

(22) Kandioller, W.; Hartinger, C. G.; Nazarov, A. A.; Kuznetsov, M. L.; John, R. O.; Bartel, C.; Jakupec, M. A.; Arion, V. B.; Keppler, B. K. From pyrone to thiopyrone ligands-rendering maltol-derived ruthenium(II)−arene complexes that are anticancer active in vitro. *Organometallics* **2009**, *28*, 4249−4251.

(23) Chen, H.; Parkinson, J. A.; Morris, R. E.; Sadler, P. J. Highly selective binding of organometallic ruthenium ethylenediamine complexes to nucleic acids: novel recognition mechanisms. *J. Am. Chem. Soc.* **2003**, *125*, 173−186.

(24) Jakupec, M. A.; Galanski, M.; Keppler, B. K. Tumour-inhibiting platinum complexes—state of the art and future perspectives. *Rev. Physiol. Biochem. Pharmacol.* **2003**, *146*, 1−53.

(25) Kandioller, W.; Hartinger, C. G.; Nazarov, A. A.; Bartel, C.; Skocic, M.; Jakupec, M. A.; Arion, V. B.; Keppler, B. K. Maltol-derived ruthenium−cymene complexes with tumor inhibiting properties: The impact of ligand−metal bond stability on anticancer activity in vitro. *Chem.—Eur. J.* **2009**, *15*, 12283−12291.

(26) Hann, S.; Koellensperger, G.; Stefanka, Z.; Stingeder, G.; Fuerhacker, M.; Buchberger, W.; Mader, R. M. Application of HPLC-ICP-MS to speciation of cisplatin and its degradation products in water containing different chloride concentrations and in human urine. *J. Anal. At. Spectrom.* **2003**, *18*, 1391−1395.

(27) Kurzwernhart, A.; Kandioller, W.; Enyedy, É. A.; Novak, M.; Jakupec, M. A.; Keppler, B. K.; Hartinger, C. G. 3-Hydroxyflavones vs. 3-hydroxyquinolinones: structure−activity relationships and stability studies on Ru^{II}(arene) anticancer complexes with biologically active ligands. *Dalton Trans.* **2012**, DOI: 10.1039/c2dt32206d.

(28) Peacock, A. F. A.; Melchart, M.; Deeth, R. J.; Habtemariam, A.; Parsons, S.; Sadler, P. J. Osmium(II) and ruthenium(II) arene maltolato complexes: rapid hydrolysis and nucleobase binding. *Chem.—Eur. J.* **2007**, *13*, 2601−2613.

(29) Luo, F. R.; Wyrick, S. D.; Chaney, S. G. Pharmacokinetics and biotransformations of oxaliplatin in comparison with ormaplatin following a single bolus intravenous injection in rats. *Cancer Chemother. Pharmacol.* **1999**, *44*, 19−28.

(30) Groessl, M.; Hartinger, C. G.; Dyson, P. J.; Keppler, B. K. CZE-ICP-MS as a tool for studying the hydrolysis of ruthenium anticancer drug candidates and their reactivity towards the DNA model compound dGMP. *J. Inorg. Biochem.* **2008**, *102*, 1060−1065.

(31) Spicer, J. A.; Gamage, S. A.; Atwell, G. J.; Finlay, G. J.; Baguley, B. C.; Denny, W. A. Structure−Activity Relationships for Acridine-Substituted Analogues of the Mixed Topoisomerase I/II Inhibitor *N*-[2-(Dimethylamino)ethyl]acridine-4-carboxamide. *J. Med. Chem.* **1997**, *40*, 1919−1929.
(32) Mendoza-Ferri, M. G.; Hartinger, C. G.; Mendoza, M. A.; Groessl, M.; Egger, A. E.; Eichinger, R. E.; Mangrum, J. B.; Farrell, N. P.; Maruszak, M.; Bednarski, P. J.; Klein, F.; Jakupec, M. A.; Nazarov, A. A.; Severin, K.; Keppler, B. K. Transferring the concept of multinuclearity to ruthenium complexes for improvement of anticancer activity. *J. Med. Chem.* **2009**, *52*, 916−925.
(33) Smith, G. S.; Therrien, B. Targeted and multifunctional arene ruthenium chemotherapeutics. *Dalton Trans.* **2011**, *40*, 10793−10800.
(34) Senderowicz, A. M. Novel direct and indirect cyclin-dependent kinase modulators for the prevention and treatment of human neoplasms. *Cancer Chemother. Pharmacol.* **2003**, *52*, S61−S73.
(35) Song, H. F.; Kerman, K.; Kraatz, H. B. Electrochemical detection of kinase-catalyzed phosphorylation using ferrocene-conjugated ATP. *Chem. Commun.* **2008**, 502−504.
(36) Martic, S.; Labib, M.; Kraatz, H. B. Enzymatically modified peptide surfaces: towards general electrochemical sensor platform for protein kinase catalyzed phosphorylations. *Analyst* **2011**, *136*, 107−112.
(37) Hanif, M.; Henke, H.; Meier, S. M.; Martic, S.; Labib, M.; Kandioller, W.; Jakupec, M. A.; Arion, V. B.; Kraatz, H.-B.; Keppler, B. K.; Hartinger, C. G. Is the reactivity of M(II)−arene complexes of 3-hydroxy-2(1*H*)-pyridones to biomolecules the anticancer activity determining parameter? *Inorg. Chem.* **2010**, *49*, 7953−7963.
(38) Larsen, A. K.; Escargueil, A. E.; Skladanowski, A. Catalytic topoisomerase II inhibitors in cancer therapy. *Pharmacol. Ther.* **2003**, *99*, 167−181.
(39) Liu, L. F. DNA topoisomerase poisons as antitumor drugs. *Annu. Rev. Biochem.* **1989**, *58*, 351−375.
(40) Nijveldt, R. J.; van Nood, E.; van Hoorn, D. E.; Boelens, P. G.; van Norren, K.; van Leeuwen, P. A. Flavonoids: a review of probable mechanisms of action and potential applications. *Am. J. Clin. Nutr.* **2001**, *74*, 418−425.
(41) Bandele, O. J.; Osheroff, N. Bioflavonoids as poisons of human topoisomerase II alpha and II beta. *Biochemistry* **2007**, *46*, 6097−6108.
(42) Holden, J. A. DNA topoisomerases as anticancer drug targets: from the laboratory to the clinic. *Curr. Med. Chem. Anti-Cancer Agents* **2001**, *1*, 1−25.
(43) Champoux, J. J. DNA topoisomerases: structure, function, and mechanism. *Annu. Rev. Biochem.* **2001**, *70*, 369−413.
(44) Dorcier, A.; Hartinger, C. G.; Scopelliti, R.; Fish, R. H.; Keppler, B. K.; Dyson, P. J. Studies on the reactivity of organometallic Ru−, Rh−, and Os−pta complexes towards DNA model compounds. *J. Inorg. Biochem.* **2008**, *102*, 1066−1076.
(45) Bennett, M. A.; Smith, A. K. Arene ruthenium(II) complexes formed by dehydrogenation by cyclohexadienes with ruthenium(III) trichloride. *J. Chem. Soc., Dalton Trans.* **1974**, 233−241.
(46) Pressprich, M. R.; Chambers, J. *SAINT+ Integration Engine, Program for Crystal Structure Integration*; Bruker Analytical X-ray Systems: Madison, WI, 2004.
(47) Sheldrick, G. M. A short history of SHELX. *Acta Crystallogr., Sect. A: Found. Crystallogr.* **2008**, *A64*, 112−122.
(48) Farrugia, L. J. ORTEP-3 for windows—a version of ORTEP-III with a graphical user interface (GUI). *J. Appl. Crystallogr.* **1997**, *30*, 565.
(49) Bracht, K.; Boubakari; Grünert, R.; Bednarski, P. J. Correlations between the activities of 19 anti-tumor agents and the intracellular glutathione concentrations in a panel of 14 human cancer cell lines: comparisons with the National Cancer Institute data. *Anti-Cancer Drugs* **2006**, *17*, 41−51.